

BOUNDING APPROACH FOR FAULT DETECTION AND DIAGNOSIS

Ioana Fagarasan⁺, Stéphane Ploix^{*}, Sylviane Gentil^{*}

⁺University "Politehnica" of Bucharest, Faculty of Control and Computers
131 Spl. Independentei, 77206 Bucharest, Romania, Phone/Fax. 4117700
email: ioana@shiva.pub.ro

^{*}Laboratoire d'Automatique de Grenoble, INPG, UJF, UMR 5528,
BP 46, F-38402 Saint Martin d'Hères Cedex, France
Phone: 33 4 76 82 62 28, Fax: 33 4 76 82 63 88
e-mail : Stephane.Ploix@inpg.fr, Sylviane.Gentil@inpg.fr

Abstract: This paper focuses on a fault detection method taking model uncertainties into account. Every uncertain parameter is represented by a bounded variable. The proposed strategy for fault detection and diagnosis consists in modeling the uncertainties, in generating output envelopes and then in testing their coherency with measurements. An application of the method was carried out on a nuclear fuel reprocessing plant simulator. A fault scenario will be presented in order to enlighten the methodology. *Copyright © 2001 IIFAC*

Keywords. Fault detection and isolation, model-based diagnosis, coherency test, set membership.

1. INTRODUCTION

Fault detection methods often use the concept of analytical redundancy based on a mathematical model of the studied system. In contrast to device redundancy, when measurements from parallel sensors are compared to each other, with model based diagnosis (Isermann, 1997) sensor's measurements are compared to analytically computed values of the respective variable, or combined into a mathematical relation (parity equation, output observer, ...). Such computations use present and/or previous measurements of other variables, and the mathematical plant model describing their nominal relationship. The computations result in residuals used to diagnose faults in the considered system. The classical tests generally rely on the fact that some residuals are near 0 and others don't. This is difficult to test in practical cases, due to modeling errors and noise; thus some authors propose statistical tests and

others use fuzzy decision making (Montmain and Gentil, 2000).

Bounding approach for fault detection is another approach, which seems to be promising because it takes into account a priori knowledge on modeling uncertainties and measurement errors. In the case of single output models, it consists in generating an output envelope using intervals as parameters model or noise model.

Interval models are useful, for example, in the following situation (Armengol *et al.*, 2000):

- the chosen model does not represent precisely the actual behavior and then the model parameters are supposed to be time varying
- the parameters of the system may vary with time, but inside bounded ranges
- the model has to be used for several similar systems that manifest differences due to the tolerance of their components.

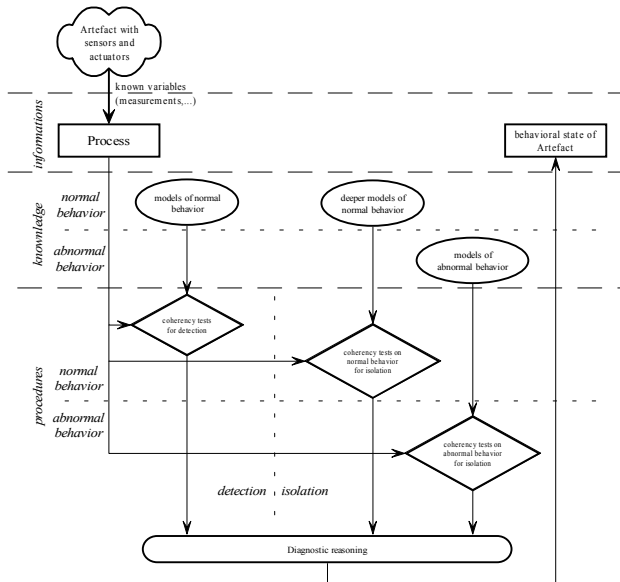


Fig. 1. Stages of model based fault diagnosis

Any diagnostic procedure is always based on coherency tests between observations and a behavioral model. Considering the model type and nature, and the way of performing coherency tests, different diagnosis procedures can be formulated.

Models may represent a normal pattern of behavior or an abnormal one, when dedicated to a specific fault (Travé-Massuyès *et al*, 1997). Models may be qualitative or quantitative, composed by a set of signatures or by relations between physical variables. In membership set approaches, the coherence is verified with the membership to an interval or, in general, to a bounded set: if the membership is not verified, the coherency test fails and it is sure that there is a fault in the system. This procedure avoids false alarms.

The model-based FDI method, as described in this paper, generally uses a structure with two theoretical stages (figure1): normal and abnormal behavior.

A drawback of set membership calculus is that, in the case of multiple outputs systems, it leads to complicated computations. For fault diagnosis of a complex process, a causal analysis allows to build-up a causal graph: each node of the graph represents a measured variable, each arc represents a dynamic link between the variables. Thus each measurement is related to its antecedents in the graph with a very simple MISO model.

The implicit hypothesis for diagnosis is that this structure provides a conceptual tool for finding useful interval analytical redundancy. The coherency tests by means of set membership studies on these simple models lead to reasonable computations (Ploix *et al.*, 2000).

In this paper, a causal representation for an industrial facility (a nuclear plant) will be presented in the

second section. The modeling of uncertainty will be detailed in the third section. Section four deals with parameter uncertainty characterization and output envelope generation. Section five describes the coherency tests on an example. A final conclusion ends the paper.

2. PROCESS REPRESENTATION

An application of the method was carried out on a nuclear fuel reprocessing plant designed to separate uranium and plutonium from fission products by selective extraction.

A simulator of the process is available and consists in a set of non-linear differential equations. It is based on a deep mathematical model of the plant, written by nuclear physicists. It can provide normal behavior and can simulate faulty behavior too (sensor, actuator and process faults). It has been designed to train operators to control and supervise the plant in various situations. In the following, and for evident safety reasons, the experiments which are presented are obtained with this simulator and not with a real faulty process.

A careful physical study of the system permitted to obtain a causal graph of this facility (Leyval *et al.*, 1994). The causal graph of the system is a special representation of block-diagrams, where all variables are measured and the block transfer functions are as simple as possible.

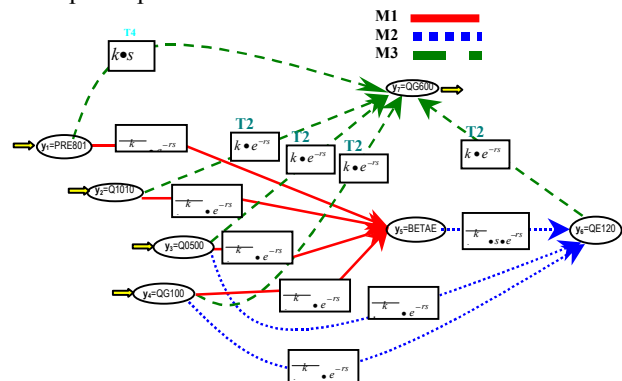


Fig. 2. A simplified causal graph for the nuclear fuel reprocessing plant

For the application described in this paper, a simplified graph is used (figure 2). It corresponds to the highest abstraction graph of the nuclear fuel reprocessing application, modeling the flow balances. The model of the plant, whose structure is given by the causal graph in figure 2, is composed of 3 elementary MISO models. Each model includes several arcs; each arc corresponds to a transfer function of one of the following type: gain with time delay, 1st order transfer function with time delay, gain with derivative and 1st order transfer function with derivative and time delay. Each parameter of the

transfer functions is supposed to belong to a bounded set represented by an interval, except for the uncertainties on time delay which are supposed to be smaller than the sample time and consequently negligible.

3. MODELLING UNCERTAINTIES

Uncertainty representation rises from the nature of the non-deterministic variable (figure 3).

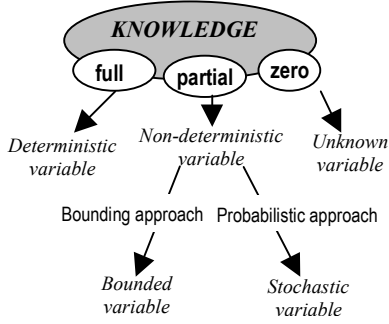


Fig. 3. Variable nature

In order to tackle models containing uncertainties by a bounding approach, it is necessary to introduce the concept of abstract space, noted as $\mathcal{A}(\cdot)$ in the following. Let x be a bounded variable; in other words it is only known by the space to which it may belong; then this space will be noted as $\mathcal{A}(x)$. If $f(\cdot)$ is a function of vector x containing abstract variables, then the abstract space of this function is determined by:

$$\mathcal{A}(f(x)) = \left[\inf_{x \in \mathcal{A}(x)} (f(x)), \sup_{x \in \mathcal{A}(x)} (f(x)) \right] \quad (1)$$

The borders of this space can be computed using the interval's arithmetic.

Noting $\mathcal{A}(v)$, the bounded set of all possible values of v , a first order transfer function with parameter uncertainties (on the gain $\rho_k\%$ and on the time constant $\rho_\tau\%$) corresponds to equation 2a:

$$\frac{dy}{dt} = -\frac{1}{(1+\rho_\tau v_\tau)\tau} y + \frac{(1+\rho_k v_k)k}{(1+\rho_\tau v_\tau)\tau} u \quad (2a)$$

where $\rho_\tau \geq 0$, $\rho_k \geq 0$ and $\mathcal{A}(v_\tau) = \mathcal{A}(v_k) = [-1 \ 1]$.

Moreover, measurement noises have to be modelled. Let \tilde{y} be the measurement of the physical variable y ; by extension the ' \sim ' sign above a variable means the variable measurement. Equation (2a) must be completed by:

$$\tilde{u} = u + \rho_u v_u \quad \text{and} \quad \tilde{y} = y + \rho_y v_y \quad (2b)$$

where $\rho_u \geq 0$, $\rho_y \geq 0$ and $\mathcal{A}(v_u) = \mathcal{A}(v_y) = [-1 \ 1]$.

Model (2) takes into account 4 different uncertainties; nevertheless, it cannot be directly used: only discrete-time models can be utilized. Consider

the following ordinary differential equation: $\dot{y} = f(y, \tilde{u}, v)$ where \tilde{u} is a vector of known variable, y the vector of variables to be calculated and v a vector of bounded variables defined by $\|v\|_\infty = 1$. At time t , $y(t)$ belong to the abstract space $\mathcal{A}(y(t))$. In order to determine y at any sample time, the set of all possible values of y at time $t+\varepsilon$ has to be evaluated from the results at time t . If ε is small enough, $\mathcal{A}(y(t+\varepsilon))$ is given by:

$$\mathcal{A}(y(t+\varepsilon)) \approx \mathcal{A}(y(t) + f(y(t), \tilde{u}(t), v(t)))$$

The right-hand expression is not equal to :

$$\mathcal{A}(y(t)) + \mathcal{A}(f(y(t), \tilde{u}(t), v(t)))$$

because both terms of the sum are correlated due to the presence of the vector $y(t)$, belonging to $\mathcal{A}(y(t))$. That means that it is not possible to evaluate the set $\mathcal{A}(y(t+\varepsilon))$ from the knowledge of $\mathcal{A}(y(t))$ and from the abstract space $\mathcal{A}(f(y(t), \tilde{u}(t), v(t)))$ stemming from the ordinary differential equation. The set $\mathcal{A}(y(t+\varepsilon))$ can only be calculated from the expression $y(t+\varepsilon)$, which amounts to use discrete time models.

Assuming that uncertain variables do not vary during a sample time, a discrete time model can be evaluated. If u comes from a zero order hold, model (2) yields

$$\begin{cases} y_{k+1} = e^{-\frac{T_e}{(1+\rho_\tau v_\tau)\tau}} y_k + k(1+\rho_k v_k) \left(1 - e^{-\frac{T_e}{(1+\rho_\tau v_\tau)\tau}} \right) \tilde{u}_k \dots \\ \dots - k(1+\rho_k v_k) \left(1 - e^{-\frac{T_e}{(1+\rho_\tau v_\tau)\tau}} \right) \rho_u v_u \\ \tilde{y}_k = y_k + \rho_y v_y \end{cases} \quad (3)$$

To calculate $\mathcal{A}(y_k) \forall k$, expression (3) will be simplified by assuming that uncertainties are small enough to be represented by a first order Taylor expansion around $v_i=0 \forall i$. Whatever the transfer function type without derivative is, the discrete-time model may be written in the form:

$$\begin{cases} y_{k+1} = (a + a_\tau v_\tau) y_k + (b + b_\tau v_\tau + b_k v_k) \tilde{u}_k + e_u v_u \\ \tilde{y}_k = y_k + \rho_y v_y \end{cases} \quad (4a)$$

If there is a derivative, the discrete-time model structure is:

$$\begin{cases} y_{k+1} = (a + a_\tau v_\tau) y_k + (b + b_\tau v_\tau + b_k v_k) (\tilde{u}_{k+1} - \tilde{u}_k) \dots \\ \dots + e_u (v_{k+1} - v_k) \\ \tilde{y}_k = y_k + \rho_y v_y \end{cases} \quad (4b)$$

To compute the set of all possible values of the measurement \tilde{y}_k , interval calculation laws (Moore, 1979) have to be used.

Table 1. Relation between uncertain continuous-time models and discrete-time models

continuous-time transfer function	discrete-time model					
	a	a_τ	b	b_τ	b_k	e_u
$\frac{(1+\rho_k v_k)k}{1+(1+\rho_\tau v_\tau)\tau p}$	$e^{-\frac{T_e}{\tau}}$	$\frac{T_e e^{-\frac{T_e}{\tau}}}{\tau} \rho_\tau$	$k \left(1 - e^{-\frac{T_e}{\tau}}\right)$	$-\frac{k T_e e^{-\frac{T_e}{\tau}}}{\tau} \rho_\tau$	$k \left(1 - e^{-\frac{T_e}{\tau}}\right) \rho_k$	$k \left(1 - e^{-\frac{T_e}{\tau}}\right) \rho_u$
$(1+\rho_k v_k)k$	0	0	k	0	$k \rho_k$	$k \rho_u$
$\frac{(1+\rho_k v_k)kp}{1+(1+\rho_\tau v_\tau)\tau p}$	$e^{-\frac{T_e}{\tau}}$	$\frac{T_e e^{-\frac{T_e}{\tau}}}{\tau} \rho_\tau$	$\frac{k}{\tau}$	$-\frac{k T_e e^{-\frac{T_e}{\tau}}}{\tau} \rho_\tau$	$\frac{k}{\tau} \rho_k$	$\frac{k}{\tau} \rho_u$
$(1+\rho_k v_k)kp$	0	0	k	0	$k \rho_k$	$k \rho_u$

The abstract space $\mathbb{A}(\tilde{y}_k)$ is obtained (Ploix and Gentil, 2000) by solving one of the two following systems depending of the presence of derivative in the transfer function.

From (4a):

$$\begin{cases} \mathbb{A}(y_0) = [\tilde{y}_0, \hat{y}_0] \\ \left[\tilde{y}_{k+1}, \hat{y}_{k+1} \right] = \begin{bmatrix} a\tilde{y}_k + b\tilde{u}_k - |a_\tau \tilde{y}_k + b_\tau \tilde{u}_k| - |b_k \tilde{u}_k| - |e_u| \\ a\hat{y}_k + b\hat{u}_k + |a_\tau \hat{y}_k + b_\tau \hat{u}_k| + |b_k \hat{u}_k| + |e_u| \end{bmatrix} \\ \mathbb{A}(\tilde{y}_k) = [\tilde{y}_k - \rho_y, \hat{y}_k + \rho_y] \end{cases} \quad (6a)$$

and from (4b):

$$\begin{cases} \mathbb{A}(y_0) = [\tilde{y}_0, \hat{y}_0] \\ \left[\tilde{y}_{k+1}, \hat{y}_{k+1} \right] = \begin{bmatrix} a\tilde{y}_k + b(\tilde{u}_{k+1} - \tilde{u}_k) - |a_\tau \tilde{y}_k + b_\tau (\tilde{u}_{k+1} - \tilde{u}_k)| \dots \\ \dots - |b_k (\tilde{u}_{k+1} - \tilde{u}_k)| - |e_u| \\ a\hat{y}_k + b(\hat{u}_{k+1} - \hat{u}_k) + |a_\tau \hat{y}_k + b_\tau (\hat{u}_{k+1} - \hat{u}_k)| \dots \\ \dots + |b_k (\hat{u}_{k+1} - \hat{u}_k)| + |e_u| \end{bmatrix} \\ \mathbb{A}(\tilde{y}_k) = [\tilde{y}_k - \rho_y, \hat{y}_k + \rho_y] \end{cases} \quad (6b)$$

Taking into account the different types of transfer function that characterize the causal model of the plant, relations in Table 1 were obtained. These relations allow calculation of the abstract spaces for each variable of the causal graph.

4. UNCERTAINTY CHARACTERISATION AND ENVELOPE GENERATION

From a practical point of view, the uncertainty characteristics have to be determined. There are two main approaches: an empirical one and a numerical one. The first one consists in utilizing physical knowledge on uncertainties and then in adjusting the additive uncertainties (e_u in equation 7) in order to remain coherent with models used for the normal behavior. The second one, that has been used in this work, consists in using algorithms given in (Ploix *et al*, 1999) and partially presented in this section.

Uncertainties on gains and time constants modelled

as a relative accuracy pattern were considered for each transfer function as follows:

$$k' = k(1 + \rho_k v_k) \quad \mathcal{A}(v_k) = [-1; 1]$$

$$\tau' = \tau(1 + \rho_\tau v_\tau) \quad \mathcal{A}(v_\tau) = [-1; 1]$$

Thanks to these structures, the characterization of uncertainties determines the ρ_k , ρ_τ and the additive error e_u , considering for the output variable \tilde{y}_k the relation:

$$\tilde{y}_k = f(\tilde{u}_k, \rho_k, \rho_\tau) + e_u ; \mathcal{A}(e_u) = [-\delta_u, \delta_u] \quad (7)$$

where \tilde{u}_k is the measurement of the input variable, i. e. the upstream node in the graph.

From each of the three models of the graph presented in figure 2, it is intended to minimize the objective function, representing the precision for each model output as follows:

$$J = \frac{\sum_{k=1}^N (\hat{y}_k - \tilde{y}_k)}{N}$$

where \hat{y}_k and \tilde{y}_k denote respectively maximum and minimum possible values for y_k .

The imposed constraints are:

$$G = \begin{bmatrix} \tilde{y}_k - \hat{y}_k \\ \tilde{y}_k - \tilde{y}_k \\ -\rho_k \\ -\rho_\tau \\ -\delta_u \end{bmatrix} \langle 0$$

These constraints ensure that the value \tilde{y}_k has to be within the borders, \tilde{y}_k and \hat{y}_k , and that the uncertainty parameters ρ_k , ρ_τ and δ_u are positive in order for the solution make sense.

The functions developed in order to describe the objective function and the constraints have been implemented using the simplex method with constraints (Fagarasan, 2000).

Using bounded variables and interval models, the response considering the given inputs is defined by two curves, \tilde{y}_k and \hat{y}_k , determined by the minimum and the maximum of the possible responses (figure 4). So, the output for such a model at a given moment is an interval instead of a certain value.

Using the relations 6a, 6b and Table 1 the envelopes (abstract spaces along time) characterizing each model can be defined and generated.

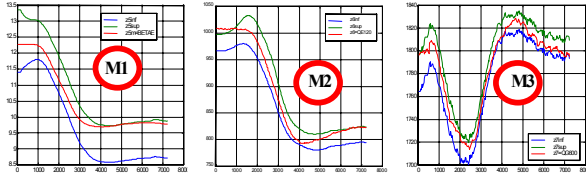


Fig. 4. Resulting envelopes of uncertainties characterization

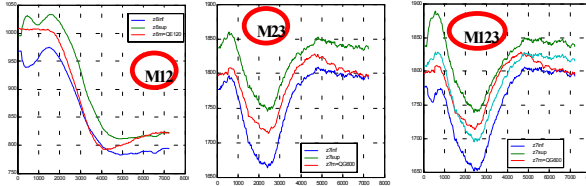


Fig. 5. Uncertainties propagation

Figure 4 shows the values of the intervals obtained for each model apart (M1, M2, M3) and figure 5 reflects the uncertainties propagation from one model to another (see figure 2, for example M12 = from M1 to M2, where z5 is deduced from M1, M23 = from M2 to M3, where z6 is deduced from M2, or M123 = from M1 to M2 and to M3, where z5 is deduced from M1 and z6 is deduced from M2). In the last mentioned case there can be observed an expansion of the interval, but not a very significant one.

Notice that the mean interval width obtained by estimating the possible values of QG600 from M3, M23 and M123 shows (figure 4 and 5) that the propagation of uncertainties from one model to

another, is not realized by summing up the uncertainties but by calculating their average; for example, the imprecision for M12 corresponds to the imprecision for M1 and M2 (not to their sum).

5. COHERENCY TESTS

No matter the adopted approach, any diagnostic procedure uses coherency tests between the observations and the models.

Two diagnostic procedures can be distinguished:

- normal operation oriented procedures (NOP), which use only knowledge about the normal behavior of the checked system;
- abnormal operation oriented procedures (AOP), which use knowledge regarding the behavior under faults.

The coherence principle is applied identically to both procedure types. With a NOP approach, the model is a reference for the normal operating behavior and the procedure allows detecting the presence of a fault. To isolate a certain fault the NOP procedure can be followed by an AOP one.

In this paper, a coherency test is realized for each model. The necessary relation to perform the tests is:

$$\tilde{y}_k \in [\hat{y}_k, \tilde{y}_k] \quad (8)$$

where the interval bounds are built-up by eq (6a) and (6b). If (8) is satisfied the coherence test reveals coherence between observations and model.

These tests have been checked for different behaviors. The coherence tests based on the elementary models M1, M2, M3 (figure 2) check the process behavior in the deepest way, so-called because these tests focus on the smallest diagnosticable subsystems of the plants, but these are not sufficient to distinguish faults on the process from sensor faults. Therefore, complementary tests

Table 2. All possible coherency tests and corresponding sensors and sub-processes checked

Model used for coherency tests	Sensors which belong to models							Results of coherency test
	PRES01	Q1010	QG100	Q0500	BETA6	QE120	QG600	
M1	1	1	1	1	1	0	0	0
M2	0	0	1	1	1	1	0	0
M3	1	1	1	1	0	1	1	1
M1+M2	1	1	1	1	0	1	0	0
M2+M3	1	1	1	1	1	0	1	1
M1+M2+M3	1	1	1	1	0	0	1	1

0 - if sensor $\notin M_i$; 1 - if sensor $\in M_i$ (0 - coherent, 1 - incoherent)

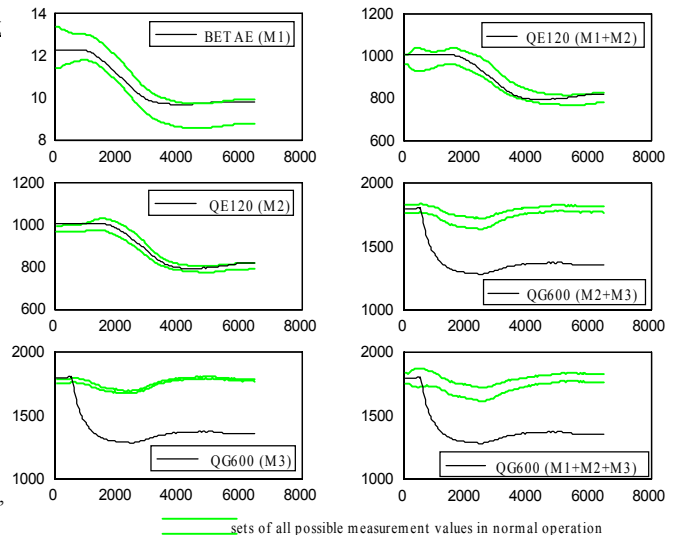


Fig. 6. Coherency tests in case of sensor fault on QG600

combining two or more models have to be proceeded.

Table 2, deduced from the causal graph (figure 2); comprises the sensors and sub-process behavior checked by coherency tests based on the different possible models. The column filled by the coherency tests is closely linked to the figure 5.

The results obtained when a fault occurs on QG600 sensor are presented in figure 6. The obtained intervals are time varying i.e. it amounts to adaptive thresholds a priori determined by the uncertainty characteristics. Looking at estimated QG600 envelopes given by models M3, M2+M3 and M1+M2+M3, it can be observed that chaining up models does not lead to important increases of uncertainties on model outputs. Coherency tests are not satisfied for models M3, M2+M3 and M1+M2+M3, and satisfied for the others as indicated in table 2, last column where 0 stands for coherency, 1 for incoherency.

Firstly, the sensors and sub-process behaviors covered by elementary models M1 M2 and M3, leading to incoherence, have to be suspected of faulty operation. At this stage, the diagnosis is that the suspected components are those which are linked to model M3, including sensors on CG1010, QG100, CQ0500, QE120 and QG600 (see table 2). Secondly, regarding the table 2, tests based on models M1, M2 and M1+M2 are coherent, then all the sensors, except the last one, QG600, provide good measurements and the sub-processes modeled by M3 may be suspected but this diagnosis has to be confirmed because a fault may be hidden at some operating mode.

Note that the first step of the strategy is sure whereas the second one has to be confirmed during different operating modes. The final diagnostic is that there are one or more faults among sensors and sub-processes, and that a fault on QG600 sensor seems to be the origin of the incoherence.

6. CONCLUSION

A new approach regarding the diagnostic procedure for uncertain systems has been presented. Interval models have been used for model parameters and noise. To decrease the complexity of interval calculus, a complex systems can be considered as interconnected elementary transfer functions, thanks to a causal analysis. The resulting model structuring arising from the principles of causal reasoning allow diagnostic procedure structuring.

Normal operation oriented diagnostic procedures used in this paper allow to generate plausible fault hypothesis. In order to refine the resulting diagnosis, it is necessary to develop faulty behavior models relied to fault hypothesis used by the abnormal operation oriented procedures. The final diagnosis is also drawn from both NOP and AOP approaches.

Compared with other strategies, the one presented in this paper has the advantage of considering the modeling uncertainties from the beginning.

The possibility of evaluating the uncertainty characteristics have been discussed, their estimation coming out from a measurement sequence representative for nominal normal behavior. All these elements lead to the improvement of knowledge regarding uncertainties. Nevertheless it has to be underlined that the uncertainty characterization has to be done very carefully because if the resulting coherency tests guarantee that there are no false alarms, it will be all the more missed faults that the output interval is overestimated.

The results for uncertainty characterization and propagation, show that the approach proposed in the present work is appropriated also in the case of complex dynamics systems, even if uncertain models are chained.

REFERENCES

- Armengol J., J. Vehi, L. Travé-Massuyès, M.A. Sainz (2000). Interval Model-based fault detection using multiple sliding time windows, 4th symposium on Fault Detection Supervision and Safety for Technical Processes, Budapest.
- Fagarasan I. (2000). Diagnostic des défaillances avec une approche ensembliste et un raisonnement causal, Rapport interne du Laboratoire d'Automatique de Grenoble, France.
- Isermann R. (1997) Supervision, fault detection and fault diagnosis methods- an introduction. *Control Engineering Practice*, 5(5):639-652.
- Leyval L., S. Gentil and S. Feray-Beaumont (1994). Model based causal reasoning for process supervision, *Automatica*, 30 (8), pp. 1295-1306.
- Montmain J., Gentil S. (2000) Dynamic causal model diagnostic reasoning for on-line technical process supervision, *Automatica* 36, 1137-1152.
- Moore R.E. (1979). Methods and applications of interval analysis, SIAM, Philadelphia, Pennsylvania.
- Ploix S., O. Adrot, J. Ragot (2000). Bounding approach to the diagnosis of a class of uncertain static systems, SAFEPROCESS 2000, Budapest, Hungary.
- Ploix S., Gentil S. (2000). *Causal strategy for set-membership fault diagnosis*, IEEE Conference on Decision and Control CDC2000, 12-15 december, Sydney (Aus).
- Ploix S., O. Adrot, J. Ragot (1999). Parameter Uncertainty Computation in Static Linear Models, Conference on Decision and Control, Phoenix, U.S.A., pp. 1916-1921.
- Travé-Massuyès L., P. Dague P., F. Guerrin (1997) *Le raisonnement qualitatif*, ed Hermès, Paris.